Journal of Molecular Structure 995 (2011) 66–71

Contents lists available at ScienceDirect

Journal of Molecular Structure

journal homepage: www.elsevier.com/locate/molstruc

Crystal structure, *ab initio* calculations and fingerprint plots of a new polymorph of *N*′,*N*″,*N*‴-triphenylbiuret

Pedro S. Pereira Silva [a,*], Raza Murad Ghalib [b], Sayed Hasan Mehdi [b], Rokiah Hashim [b], Othman Sulaiman [b], Manuela Ramos Silva [a]

[a] *CEMDRX Physics Department, University of Coimbra, P-3004-516 Coimbra, Portugal*
[b] *School of Industrial Technology, Universiti Sains Malaysia, 11800 Pulau Pinang, Malaysia*

ARTICLE INFO

Article history:
Received 26 February 2011
Received in revised form 24 March 2011
Accepted 24 March 2011
Available online 31 March 2011

Keywords:
Triphenylbiuret
Polymorphism
Ab initio calculations
Relative conformational energies
Fingerprint plots

ABSTRACT

A new polymorph of *N*′,*N*″,*N*‴-triphenylbiuret, $C_{20}H_{17}N_3O_2$ (form II), has been synthesized and the structure has been solved by X-ray diffraction. The crystals are monoclinic, space group $P2_1/c$, with $a = 7.6966(3)$ Å, $b = 12.5490(4)$ Å, $c = 18.5996(6)$ Å, $\beta = 107.632(2)°$, $Mr = 331.37$, $V = 1712.04(10)$ Å^3, $Z = 4$ and $R = 0.0454$. The hydrogen bonding of this polymorph is considerably different from that of the previously known structure. The molecules are linked in infinite chains, via C–H···O hydrogen bonds and there is also an intramolecular N–H···O hydrogen bond.

The intermolecular interactions present in this polymorph, and on the previously reported polymorph, were analysed by means of the fingerprint plots derived from the Hirshfeld surfaces. The fingerprint plots evidenced the different packing modes of the two structures.

Quantum–mechanical *ab initio* calculations for the free molecule were performed using the Hartree–Fock and DFT/B3LYP methods with the 6-31G(d,p) basis set of wave functions. The solid-state conformations compared with those obtained theoretically from DFT calculations for the isolated molecules show significant differences.

Some difficulties of using quantum–mechanical calculations for the determination of relative conformational energies are also discussed.

1. Introduction

The interest in polymorphism is rapidly growing because of its importance in industrial processes, namely in the pharmaceutical industry, since different physical properties of polymorphs can substantially alter the durability, solubility and bioavailability of the pharmaceutical drugs [1]. Conformationally flexible molecules have more degrees of freedom than rigid molecules, so a greater scope for polymorphism might be expected. The energies involved in rotating parts of the molecule about single bonds are comparable to the energy differences observed between polymorphs and so it is not surprising that molecules with torsional degrees of freedom, such as the title compound, can exhibit different conformational polymorphs.

In this article we present the crystal structure of a new polymorph of *N*′,*N*″,*N*‴-triphenylbiuret and we compare it with the previously known structure [2] using several computational tools.

In this work we used the CrystalExplorer software [3] to calculate the 2D fingerprint plots, to elucidate the different crystal environments of the two polymorphs. Such graphical tools based on Hirshfeld surfaces [4,5] and on the derived two-dimensional (2D) fingerprint plots [6,7] are a valuable tool for visualizing and analyzing intermolecular interactions in polymorphs and make the task of polymorph discrimination considerably easier.

We have also calculated the energies of the two solid state conformations of triphenylbiuret known so far and several methods of calculating the relative energy were compared.

2. Experimental and computational methods

2.1. Preparation of the title compound

A mixture of Phenyl isocyanate (1.08 ml, 10 mmol) and diethyl malonate (1.51 ml, 10 mmol) in molar ratio 1:1 were refluxed in THF on a water bath for 6 h in the presence of Na_2CO_3 (Scheme 1). The reaction mixture was dried on rota vapour at low pressure and further fractionated with chloroform.

The chloroform soluble part was further dried on rotavapor and chromatographed over silica gel (Merck, 0.04–0.063 mm, 230–400

---

* Corresponding author. Tel.: +351 239 410 652; fax: +351 239 829 158.
E-mail addresses: psidonio@pollux.fis.uc.pt, pedro.sidonio@gmail.com (P.S. Pereira Silva).

0022-2860/$ - see front matter © 2011 Elsevier B.V. All rights reserved.
doi:10.1016/j.molstruc.2011.03.057

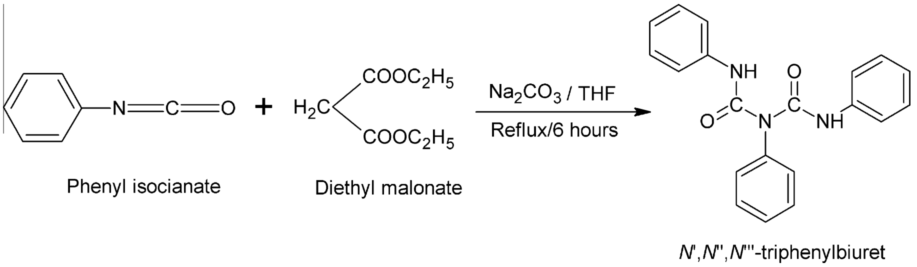

Scheme 1. Synthesis route.

mesh ASTM) column loaded in light petroleum ether. The column was eluted successively with light petroleum ether and light petroleum ether–diethylether (9:1–1:1). The elutants obtained in solvent system light petroleum ether–diethylether (9:1–8:2), on crystallization with chloroform–*n*-hexane (1:1), gave the transparent crystals of *N*′,*N*″,*N*‴-triphenylbiuret (550 mg) (mp. 148 °C). The melting point was determined on a Thermo Fisher digital melting point apparatus of IA9000 series. The polymorph reported by Carugo et al. [2] was obtained with a reaction of triethylindium with an excess of phenyl isocyanate, as described by Tada & Okawara [8].

2.2. Crystal structure determination

A crystal of (form II) with a block shape and having approximate dimensions of 0.40 mm × 0.32 mm × 0.25 mm was glued on a glass fibre and mounted on a Bruker Apex II diffractometer. Diffraction data were collected at room temperature 293(2) K using graphite monochromated Mo Kα ($\lambda = 0.71073$ Å). Data reduction was performed with APEX II [9]. Lorentz and polarization corrections were applied. Absorption correction was applied using SADABS [10]. The crystallographic structure was solved by direct methods (SHELXS-97) [11]. Refinements were carried out with SHELXL-97 package [11]. All refinements were made by full-matrix least-squares on F^2, with anisotropic displacement parameters for all non-hydrogen atoms. All the hydrogen atoms could be located in a difference Fourier synthesis but they were placed at calculated positions and then, included in the structure factor calculation in a riding model using SHELXL-97 defaults. The final least-squares cycle was based on 4521 observed reflections [$I > 2\sigma(I)$], 226 variable parameters, converged with $R = 0.0454$ and $wR = 0.1096$. Additional information to the structure determination is given in Table 1. Selected structural parameters can be seen in Table 2. Hydrogen bond geometric data is given on Table 3. Supplementary data have been deposited at the Cambridge Crystallographic Data Centre (CCDC No. 795370).

2.3. Ab initio calculations

Ab initio studies using the Firefly QC package [12], which is partially based on the GAMESS (US) source code [13], were performed to calculate the energy differences between conformers. Various constraints were imposed during the calculations to determine the best methodology for calculating the relative energies.

Usually, single point calculations on each polymorph are considered the best measure of relative energy. However, small differences in the experimental bond lengths and angles between the conformers will lead to large energy differences [14].

The different methods used in the *ab initio* calculations were the following

(1) The single point energy for the experimental X-ray geometries (ΔE^{crys});

Table 1
Crystallographic data and structure refinement of the title compound (form II).

Empirical formula	$C_{20}H_{17}N_3O_2$
Formula weight	331.37
Temperature (K)	293(2)
Wavelength (Å)	0.71073
Crystal system	Monoclinic
Space group	$P2_1/c$
a (Å)	7.6966 (3)
b (Å)	12.5490 (4)
c (Å)	18.5996 (6)
β (°)	107.632(2)
Volume (Å^3)	1712.04 (10)
Z	4
Calculated density (g/cm^3)	1.286
Absorption coefficient (mm^{-1})	0.085
F(0 0 0)	696
Crystal size (mm)	0.40 × 0.32 × 0.25
θ range for data collection (°)	2.78 –26.82
Index ranges	$-10 < h < 10$, $-16 < k < 17$, $-24 < l < 24$
Reflections collected/unique	34706/4521 [*R*(int) = 0.0260]
Completeness to *θ* = 25.00°	99.9%
Refinement method	Full-matrix least-squares on F^2
Data/restraints/parameters	4521/0/226
Goodness-of-fit on F^2	1.003
Final *R* indices [$I > 2\sigma(I)$]	*R1* = 0.0454 *wR2* = 0.1096
R indices (all data)	*R1* = 0.0796 *wR2* = 0.1312
Largest diff. peak and hole (e Å^{-3})	0.168 and −0.208

Table 2
Comparison of selected geometrical parameters for form II and form I as determined by X-ray diffraction and from DFT calculations (Å, °).

	Experimental		DFT	
	Form II	Form I	Form II	Form I
O1–C1	1.2201(16)	1.2197(15)	1.2334	1.2333
O2–C2	1.2055(17)	1.2134(17)	1.2209	1.2206
N1–C1	1.3965(17)	1.4122(18)	1.4106	1.4097
N1–C2	1.4255(17)	1.4275(17)	1.4491	1.4483
N1–C3	1.4463(17)	1.4472(16)	1.4458	1.4468
N2–C1	1.3540(17)	1.3505(17)	1.3695	1.3699
N2–C9	1.4190(18)	1.4230(18)	1.4144	1.4140
N3–C2	1.3404(17)	1.3400(16)	1.3589	1.3596
N3–C15	1.4136(17)	1.4184(19)	1.4099	1.4098
C1–N1–C2	124.94(11)	123.92(12)	125.66	125.69
C1–N1–C3	120.65(11)	120.53(12)	120.56	120.56
C1–N2–C9	123.80(12)	126.11(12)	128.52	128.57
C2–N3–C15	126.67(12)	126.96(14)	127.31	127.37
N2–C1–N1	114.75(12)	113.94(12)	114.24	114.30
N3–C2–N1	115.90(12)	116.24(14)	115.29	115.29
C1–N1–C3–C4	−88.22(18)	−68.26(19)	−90.33	−89.59
C1–N2–C9–C14	50.5(2)	−6.6(2)	2.38	−1.51
C2–N1–C3–C8	−89.06(17)	−72.33(19)	−90.90	−90.38
C2–N3–C15–C16	−154.59(15)	−167.13(17)	−179.67	179.67
N1–C1–N2–C9	−179.83(14)	177.07(13)	179.90	−179.91
N1–C2–N3–C15	167.26(14)	175.63(15)	179.54	−179.88
N2–C1–N1–C2	−172.99(13)	163.15(13)	−178.99	179.90
N3–C2–N1–C1	−4.3(2)	10.3(2)	−0.52	−0.19

Table 3
H-bond geometry (Å, °).

	D–H	H···A	D···A	D–H···A
C16–H16···O2^i	0.93	2.55	3.162(2)	124
N3–H3···O1 (intra)	0.86	1.91	2.593(2)	135
C20–H20···O2 (intra)	0.93	2.37	2.903(2)	116

Symmetry code *i*: $1 - x, y - 1/2, 3/2 - z$.

(2) The single point energy for the X-ray geometries with the positions of the hydrogen atoms in form I modified to be like those in form II (ΔE^1), i.e., with the same distances to the parent atoms as in form II;

(3) Energy for the structures with all parameters optimised except the torsion angles chosen to define each conformer (ΔE^2).

These calculations were performed with the molecular orbital HF method and within DFT using B3LYP (Becke three-parameter Lee–Yang–Parr) for exchange and correlation, which combines the hybrid exchange functional of Becke [15,16] with the correlation functional of Lee, Yang and Parr [17]. The calculations were performed with a 6-31G(d,p) basis set. For the method ΔE^1 we also performed HF and DFT calculations with the augmented basis set 6-311+G(d,p).

We performed also geometry optimizations starting from the experimental X-ray geometries of the two conformers. These optimizations were performed only within DFT (B3LYP for exchange and correlation and 6-31G(d,p) basis set). Tight conditions for convergence of both the self-consistent field cycles and the maximum density and energy gradient variations were imposed (10^{-5} atomic units) in both calculations. At the end of these geometry optimizations we conducted Hessian calculations to guarantee that the final structures correspond to true minima, using the same level of theory as in the geometry optimizations.

3. Results and discussion

3.1. Crystal structure

In an attempt to synthesize a totally different compound we obtained serendipitously a second polymorph, form II, of *N′,N″,N‴*-triphenylbiuret. It is monoclinic, like the already known form [2], form I, and has the same space group ($P2_1/c$) but a less extensive hydrogen-bonding arrangement. In the biuret moiety the individual –NH–CO–N– groups are planar within the standard error and the angle between these groups is considerably smaller [5.8(1)°] than the corresponding angle in form I [12.8(2)°]. The N1–C3 bond is significantly longer [1.4463(17) Å] than the N2–C9 and N3–C15 bonds [1.4190(18) and 1.4136(17) Å] (see Fig. 1).

The N3–C2 [1.3404(17) Å] and N2–C1 [1.3540(17) Å] bond lengths are in the expected range for delocalized C–N bonds [18]. The geometry around the N1 atom is the expected for a hybridized sp^2 atom.

While in the form I the phenyl rings C9–C14 and C15–C20 are roughly coplanar with the least squares plane of the biuret moiety [with dihedral angles of 11.6 (2)° and 10.9 (2)°, respectively], in this new polymorph they are considerably out of this plane, with the dihedral angles being 50.31(5)° and 21.58(6)° respectively. The ring C3–C8 is almost perpendicular to the biuret fragment [dihedral angle of 87.98(5)° between the two planes] and this can be explained by the steric hindrance of N2–H2.

The molecules are linked in infinite chains running parallel to the *b* axis, via C–H···O hydrogen bonds [Fig. 2; Table 3]. These chains have a periodicity of six atoms, graph-set symbol C(6) according to Etter's graph-set theory [19,20]. In this polymorph there is also an intramolecular N–H···O hydrogen bond with geometry similar to that found in form I [see Table 3], forming six-membered rings with graph-set symbol S(6) [19,20]. Of the two intramolecular C–H···O hydrogen bonds present in form I (C13–H13···O2; C20–H20···O2) only the C20–H20···O2 is present in this polymorph since the ring C9–C14 is considerably out of the biuret plane, not allowing a conventional hydrogen bond between the atoms C13 and O2.

The use of available strong hydrogen bond donors and acceptors is almost axiomatic [19], so an unusual structural feature in form II is the absence of the expected N2–H2···O1 hydrogen bond, that is present in form I.

The molecular packing is also influenced by several C–H···π interactions. The strongest C–H···π interaction is of the type II as described by Malone et al. [21], with a H···π^i distance of 2.81 Å, and a C–H···π angle of 162° [symmetry code: (i) $1 + x, y, z$]; the H8 atom is being attracted in the direction of the centre of the aromatic ring C15–C20. In the other two relevant C–H···π interactions, the hydrogen atoms H17 and H12 are above the centre of the phenyl ring C3–C8 but the C–H bonds point towards the ring edge. These two interactions are of the type III according to the classification of Malone et al. [21], the first with a H17···π^{ii} distance of 2.83 Å, and a C17–H17···π angle of 149° [symmetry code: (ii) $1 - x, -1/2 + y, 3/2 - z$] and the second with a H12···π^{iii} distance of 3.02 Å, and a C12–H12···π angle of 143° [symmetry code: (iii) $3 - x, 1 - y, 2 - z$].

3.2. Fingerprint plots

When comparing the same molecule in different crystal environments, Hirshfeld surfaces and fingerprint plots [4–7] have been shown to be a powerful tool for elucidating and comparing intermolecular interactions, complementing other tools currently available for the visualization of crystal structures and for their systematic description and analysis, e.g. graph-set analysis [19] and topological analysis [22].

The intermolecular interactions of this new polymorph and of the previously reported [2] were analyzed using the two-dimensional fingerprint plots [6,7] derived from Hirshfeld surfaces [4,5], using the software CrystalExplorer, version 2.1 [3]. 2D-fingerprint plots were generated by using the d_i and d_e pairs measured on each individual spot of the calculated Hirshfeld surface. Fig. 3 shows unambiguously that different intermolecular interactions are present in the polymorphs form II and form I, which result in different packing modes. In the plot of form II the 'wings' are more pronounced which indicate aromatic interactions, namely C–H···π contacts. Only the 2D-fingerprint plot of the form I shows the presence of a pair of long sharp spikes, a characteristic of the strong hydrogen bonds, in this case the N–H···O hydrogen bonds. There is evidence of close intermolecular H···H contacts in both polymorphs, that occur as a characteristic hump in the region $d_i = d_e = 1.2$ Å of the plot.

3.3. Results of the ab initio calculations

Using the three methods described previously we have performed the calculation of the energy differences between the two conformers of the title compound. The results are presented on Table 4. As expected, the results obtained using method ΔE^{crys} (single point energy for the experimental X-ray geometries) lead to very large differences of energy between the two conformations, and the major source of these differences seems to be the hydrogen atomic positions, since in our structure the hydrogen atoms were positioned geometrically and in the previously reported polymorph they were refined freely, leading to large differences in the X–H bond lengths between the two structures. The energy dif-

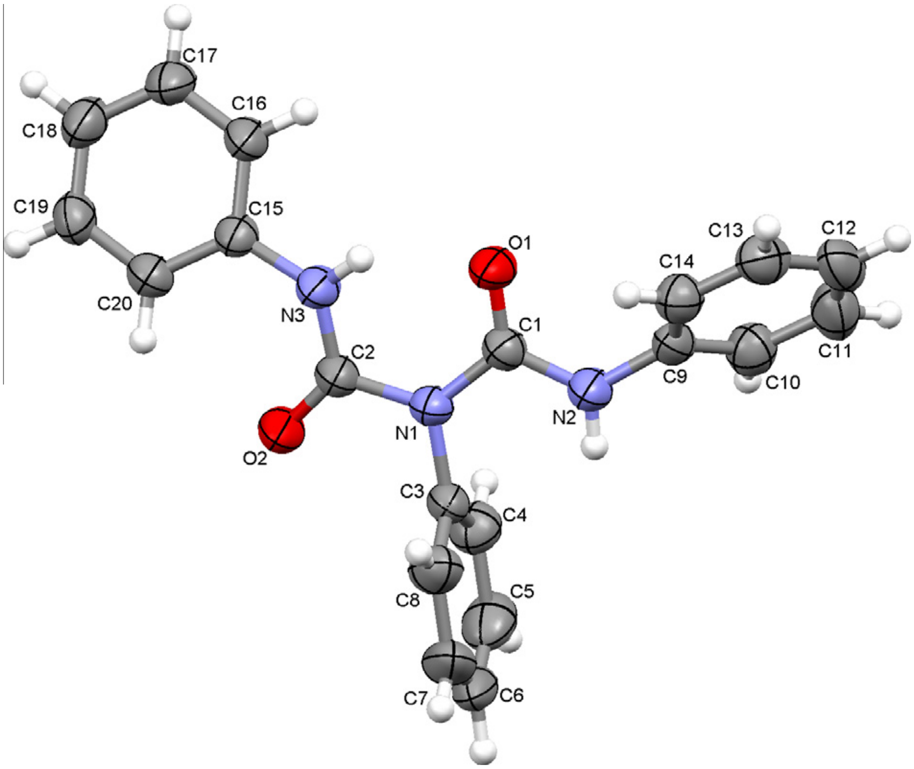

Fig. 1. Diagram of the title compound with the ellipsoids drawn at the 50% probability level, with the atomic labelling scheme (Mercury, version 2.3 [24]).

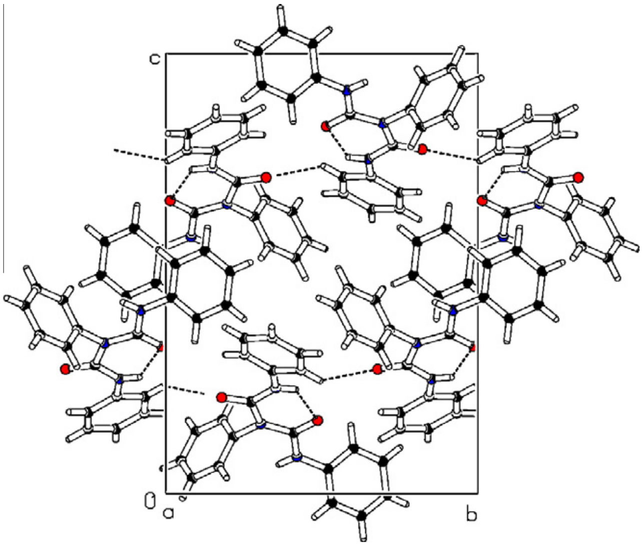

Fig. 2. Packing diagram of form II, with the H-bonds shown as dashed lines.

ferences obtained with methods ΔE^1 and ΔE^2 are much closer to typical literature values (<5 kcal mol^{-1}) [23], especially for method ΔE^2. The rotations about single bonds (intramolecular torsions) are worth 1–3 kcal mol^{-1} but can be as high as 8 kcal mol^{-1} due to steric factors or restricted rotation [14], so in the title compound we can expect energy differences of this order of magnitude.

In method ΔE^1 the hydrogen atomic positions are changed in the conformation of form I to match exactly those of conformation of form II. However, other small differences in the remaining bond lengths and angles can still be a source of errors.

Calculating the Root Mean Square Deviations (Mercury software [24]) between the X-ray geometries of both polymorphs and the optimized structure we can see that the conformation of form I is closer to the equilibrium geometry: RMSD(form II-opt) = RMSD(-form I-opt)= I-opt) ce:hsp sp="0.25"/>= ce:hsp sp="0.25"/>0.3803. According to this, we expect that the conformation of form I should be more stable than the form II conformation and thus, the method ΔE^2 (energy for the structures with all parameters optimised except torsion angles) seems to be more sensible than the other two methods used.

In order to gain some insight of the influence of the intermolecular interactions on the molecular geometry, namely the relative orientation of the phenyl rings, we have performed DFT calculations of the equilibrium geometry of the free molecule starting from the experimental X-ray geometries of the two conformers of both forms II and I. The two equilibrium geometries obtained are almost equal (see Table 2) and it can be seen that the DFT calculations reproduce well the observed experimental bond lengths and valency angles of the two conformers but some of the calculated dihedral angles in the free molecule differ significantly from the experimental (Table 2).

The differences between the calculated and experimental bond lengths are smaller than 0.0236 Å and 0.0208 Å, for the form II and the form I conformers, respectively. The largest disagreement between the experimental and calculated angle values correspond to the angle C1–N2–C9, which has a considerably smaller value in both crystals.

In the optimized structure, the rings C9–C14 and C15–C20 are almost in the plane of the biuret moiety and the ring C3–C8 is perpendicular to this plane (Table 5). Looking at the geometries of the two polymorphs (Fig. 4), the most obvious deviation from the equilibrium geometry of the free molecule is the large rotation of the ring C9–C14 from the biuret plane, in form II, and this cannot be explained by the hydrogen bonds since this ring does not participate in any hydrogen bond. However when looking for $\pi\cdots\pi$ interactions, one finds that form II has nine of these interactions with a distance between ring centroids, d_{c-c}, smaller than 6 Å and an angle

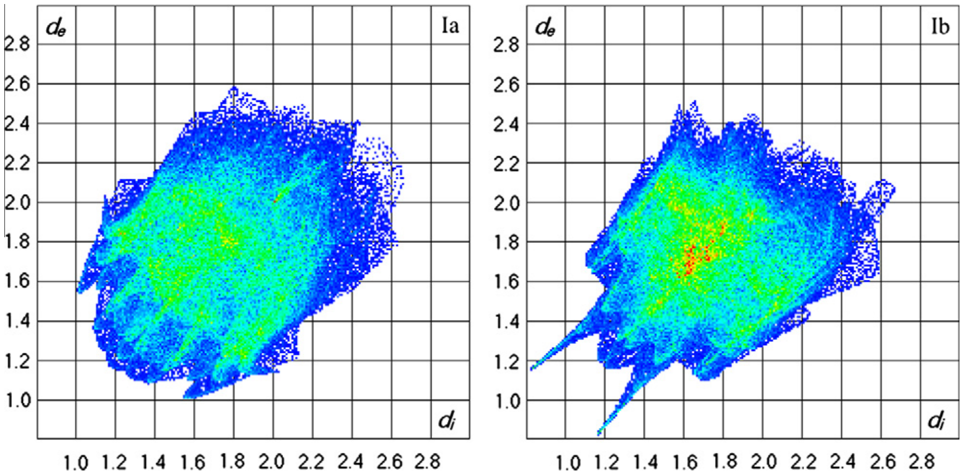

Fig. 3. Two-dimensional fingerprint plot for the forms II and I.

Table 4
Results of *ab initio* calculations, with energies (au[a]) and relative conformational energies (kcal mol^{-1}).

Method	HF/6-31G(d,p)			B3LYP/6-31G(d,p)		
	Form II	Form I	ΔE	Form II	Form I	ΔE
ΔE^{crys}	−1080.09944	−1080.31151	133.07	−1086.75497	−1086.98430	143.90
ΔE^1	−1080.09944	−1080.07680	−14.21	−1086.75497	−1086.73690	−11.34
ΔE^2	−1080.42104	−1080.42448	2.16	−1087.12204	−1087.12840	3.99
	HF/6-311+G(d,p)			B3LYP/6-311+G(d,p)		
ΔE^1	−1076.87632	−1076.85727	−11.95	−1083.65124	−1083.63724	−8.78

[a] 1 au = 627.47237 kcal mol^{-1}.

Table 5
Dihedral angles between the least-square planes of the phenyl rings and the plane of the biuret moiety for the experimental and optimized geometries.

Phenyl ring	C3–C8	C9–C14	C15–C20
Form II	88.0(1)	50.3(1)	21.6(1)
Form I	72.9(1)	11.6(1)	10.9(1)
Opt. form II	89.5	2.4	0.8
Opt. form I	90.0	1.5	0.4

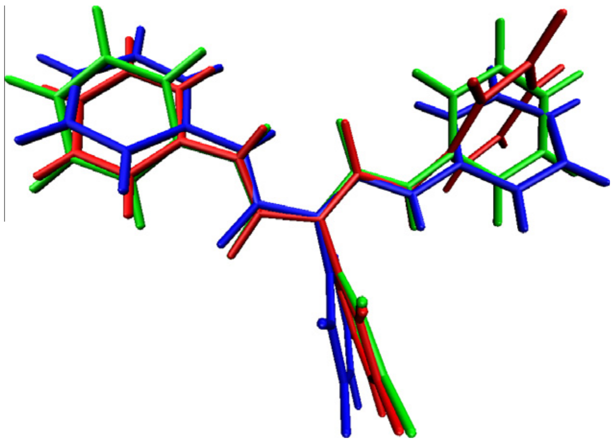

Fig. 4. Comparison of the molecular conformation of form II, as established from the X-ray study (red) with the X-ray geometry of form I (blue) and with the optimized geometry (green) (Software used for visualization: VMD, version 1.8.6, April 7, 2007 [25]). (For interpretation of the references to colour in this figure legend, the reader is referred to the web version of this article.)

β smaller than 60° (β is the slipping angle defined by the vector c1–c2, from the first ring centroid to the second and the normal to the plane of the first ring) and the phenyl ring C9–C14 participates in six of these interactions with the strongest [d_{c-c} = 3.929(1) Å] being between C9–C14 rings of two neighbouring molecules. In the form I the π···π interactions are generally weaker.

It is difficult to quantify the influence of each interaction but it is known that in typical cases, a crystal form with favourable single bond torsion finds an alternative polymorph where a slightly disfavoured torsional geometry is compensated by better interactions [23]. The latter situation is that of form II where the rotations of the phenyl rings from the equilibrium positions may be explained by the aromatic interactions (C–H···π and π···π).

The conformational energy difference between form II and form I is small and can be balanced by improved crystal packing as may be the case of the new form II which has a slightly more efficient close packing. Such packing corresponds to more and stronger short non-bonding intermolecular contacts than in the previously reported form.

4. Conclusions

A new polymorph of *N′*,*N″*,*N‴*-triphenylbiuret was crystallized and the structure was determined using single crystal X-ray diffraction. This structure was compared to the previously reported polymorph and the fingerprint plots of the two structures were derived from the Hirshfeld surfaces to analyse the intermolecular interactions. The major difference between the two polymorphs is the presence/absence of the N–H···O intermolecular hydrogen bond. The DFT geometry optimizations suggest that the supramolecular aggregation plays an important role in stabilizing the observed geometries of the two polymorphs. Compared *ab initio* calculations of conformational energies show that the positioning of the hydrogen atoms may be a source of large errors, and that extreme care should be taken in order to obtain significant results.

5. Supplementary material

Crystallographic data for the structure reported in this paper have been deposited with the Cambridge Crystallographic Data Center number, CCDC 795370. Copies of this information may be obtained free of charge on application to CCDC, 12 Union Road, Cambridge CB2 1EZ, UK (fax: +44 1223 336 033; e-mail: deposit@ccdc.cam.ac.uk or http://www.ccdc.cam.ac.uk).

Acknowledgements

We would like to acknowledge Universiti Sains Malaysia (USM) for the University Grant 1001/PTEKIND/8140152 to Dr. Raza Murad Ghalib and Dr. Sayed Hasan Mehdi. P.S. Pereira Silva acknowledges the support by Fundação para a Ciência e a Tecnologia, under the scholarship SFRH/BD/38387/2008.

References

[1] J. Bernstein, Polymorphism in Molecular Crystals. IUCr Monographs on Crystallography, Oxford University Press, Oxford, 2002.
[2] O. Carugo, G. Poli, L. Manzoni, Acta Cryst. C 48 (1992) 2013.
[3] S.K. Wolff, D.J. Grimwood, J.J. McKinnon, D. Jayatilaka, M.A. Spackman, CrystalExplorer 2.1, University of Western Australia, Perth, 2007.
[4] M.A. Spackman, P.G. Byrom, Chem. Phys. Lett. 267 (1997) 215.
[5] J.J. McKinnon, A.S. Mitchell, M.A. Spackman, Chem. – Eur. J. 4 (1998) 2136.
[6] J.J. McKinnon, M.A. Spackman, A.S. Mitchell, Acta Cryst. B 60 (2004) 627.
[7] M.A. Spackman, D. Jayatilaka, CrystEngComm 11 (2009) 19.
[8] H. Tada, R. Okawara, J. Org. Chem. 35 (1970) 1666.
[9] Bruker, APEX2 and SAINT, Bruker AXS Inc., Madison, Wisconsin, USA, 2003.
[10] G.M. Sheldrick, SADABS. University of Göttingen, Germany, 2003.
[11] G.M. Sheldrick, Acta Cryst. A 64 (2008) 112.
[12] A.A. Granovsky, PC GAMESS/Firefly version 7.1.F, 2009. <http://classic.chem.msu.su/gran/gamess/index.html>.
[13] M.W. Schmidt, K.K. Baldrige, J.A. Boatz, S.T. Elbert, M.S. Gordon, J.J. Jensen, K. Koseki, N. Matsunaga, K.A. Nguyen, S. Sue, T.L. Windus, M. Dupuis, J.A. Montgomery, J. Comput. Chem. 14 (1993) 1347.
[14] D. Buttar, M.H. Charlton, R. Docherty, J. Starbuck, J. Chem. Soc. Perkin Trans. 2 (1998) 763.
[15] A.D. Becke, Phys. Rev. A 38 (1988) 3098.
[16] A.D. Becke, J. Chem. Phys. 98 (1993) 5648.
[17] C. Lee, W. Yang, R.G. Parr, Phys. Rev. B 37 (1988) 785.
[18] G. Gilli, V. Bertolasi, F. Bellucci, B. Fabrizio, V. Ferretti, J. Am. Chem. Soc. 108 (1986) 2420.
[19] M.C. Etter, Acc. Chem. Res. 23 (1990) 120.
[20] J. Bernstein, R.E. Davis, L. Shimoni, N.-L. Chang, Angew. Chem. Int. Ed. Engl. 34 (1995) 1555.
[21] J.F. Malone, C.M. Murray, M.H. Charlton, R. Docherty, A.J. Lavery, J. Chem. Soc. Faraday. Trans. 93 (1997) 3429.
[22] V.A. Blatov, Acta Cryst. A 62 (2006) 356.
[23] A. Nangia, Acc. Chem. Res. 41 (2008) 595.
[24] C.F. Macrae, P.R. Edgington, P. McCabe, E. Pidcock, G.P. Shields, R. Taylor, M. Towler, J. van de Streek, J. Appl. Crystallogr. 39 (2006) 453.
[25] W. Humphrey, A. Dalke, K. Schulten, J. Mol. Graph. 14 (1) (1996) 33.